Genesis Of Bensa Kaolin Deposit, Southern Ethiopia; Assessment From Major And Trace Element Geochemistry Of The Kaolin Deposit

Andualem Getaw, Selamawit Dagnachew, Eyob Abebe

Abstract: Bensa kaolin deposit is found in Southern nation nationality and people of Ethiopia regional state which is 405km south of Addis Ababa, Ethiopia. This study presents new major and trace element chemistry of Bensa kaolin deposit to assess element characteristics during kaolinisation processes and genesis of the kaolin deposit of the area. Bensa kaolin is a result of weathering of rhyolitic ignimbrite and it shows high concentration of SiO_2 ranges between 53.6 to 68.8 wt. % and Fe_2O_3 (4.85-7.74 wt. %) and exhibits very limited CaO (0.27-0.62 wt. %), MgO (0.14-0.31 wt. %), P_2O_5 (0.1-0.2 wt. %) and MnO (0.12-0.3 wt. %). The highly mobile Large ion lithophile element (LILE) Sr (23.3-60.5ppm), Rb (32.3-88.4ppm), Ba (201-593ppm) and Cs (0.54-1.67ppm) of Bensa kaolin shows depletion pattern on the Chondrite normalized spider plot whereas the immobile High field strength element (HFSE) Zr (1070-1770ppm), Hf (26.8-45.4ppm), Nb (143-30ppm), Ta (9.3-14.8ppm) and REE concentrations of Bensa kaolin samples exhibit enrichment pattern. The major and trace element concentration of Bensa kaolin indicates samples from depth >20m and from the periphery of the deposit are less mature with respect to chemistry and physical property compared with samples from the center of the deposit. The depletion of CaO, MgO, P_2O_5, MnO and LILE and the enrichment of HFSE of Bensa kaolin indicates the mobile elements have been removed from the system during the kaolinisation processes and it is the characteristics of supergene kaolin origin. Under very high temperature to some extent HFSE Zr can be mobilized and it can be removed from the system but the very high concentration of Zr in Bensa kaolin deposit reflect that the kaolinisation processes may have been undertook at low temperature condition.

Index Terms: alteration, element mobility, genesis, kaolinisation, Supergene

1 INTRODUCTION

Kaolin is white to dull color low iron aluminous silicate clay mineral, formed by weathering and hydrothermal alteration of granitic and feldspatic rocks [1], [2]. Kaolin deposit can be a primary or secondary deposit. Primary deposits formed by hydrothermal alteration (hypogene kaolin) or weathering (supergene kaolin) of in-situ crystalline feldspatic igneous or metamorphic rocks while secondary kaolin deposits are a sedimentary origin [3], [4], [5], [6], [7]. Kaolin physical property is mainly depends on its chemical and physical property. Kaolin mainly composed of oxygen, silicon, aluminum, iron, and hydroxyl groups. Physically kaolin is white to nearly white color and fine grain sticky plastic touch. Iron concentration in the kaolin deposit primarily dictates its natural color [8]. Degree of alteration and maturity of a kaolin deposit can be determined by the chemical compression between the host rock and the kaolin deposit itself. Kaolin deposit formed by weathering processes shows higher silica (SiO_2) content in the kaolin which reflects lower degree of alteration of the host/parent rock [9]. The lower SiO_2 and higher Al_2O_3 in kaolin deposit are due to intense degree of alteration/weathering of the parent rock [10]. According to A. Njoya et al. [10] sandy kaolin shows high content of SiO_2 (>60%) and lower Al_2O_3 (20-25%) whereas low sandy/mature kaolin exhibits lower SiO2 (45-49%) and higher Al_2O_3 due to high kaolinite content. Weathering/supergene kaolin show a complete loss of highly mobile elements MgO, MnO, CaO and Na_2O which is the effect of kaolinisation process [11], [13], [10].

- *Andualem Getaw Addis Ababa Science and Technology University, Department of Geology, P.O. Box 16417, Addis Ababa, Ethiopia; Email-andualem.getaw@aastu.edu.et*
- *Eyob Abebe Hawasa University, Department of Geology Hawasa Ethiopia*
- *Selamawit Dagnachew Ethiopian Energy Authority Addis Ababa Ethiopia*

Chemical index of weathering (CIW) and chemical index of alteration (CIA) of any deposit can be used to determine the degree of transformation of k-feldspar and micas in to clay mineral; the high CIW and CIA value (>80) of any kaolin deposit shows the extreme degree of silicate weathering and it in turn tells us the degree of maturity of the deposit [12]. The mathematical calculation of CIA only defer that of CIW, CIW did not take K_2O in to account. The mathematical approach used to determine both chemical indexes are; CIW = $[Al_2O_3/(Al_2O_3 + CaO + Na_2O)]$ x 100 [14] and CIA = $[Al_2O_3/(Al_2O_3 + CaO + Na_2O + K_2O)]$ x100 [15]. Trace element concentrations of kaolin deposits are very important indicators whether the deposits are hypogene or supergene. In supergene kaolin highly mobile elements (Sr, Rb, Ba, U and Cs) will be leached out from the system during early stage of weathering processes [16], [17]. On the contrary immobile elements like Ti, Hf, Zr and REE remained in the residual kaolin deposit during the alteration processes [17]. Higher content of Ba+Sr in the kaolin deposit is a characteristic of hypogene kaolin whereas lower content of Ba, Sr and the higher value of Ce+Y+La are attributed to that of supergene kaolin deposits [18], [19]. Different regional geological and geochemical investigations of kaolin deposit in different parts of Ethiopia have been conducted to assess their industrial applications [20], [21], [7]. This work intends to investigate the physical and geochemical (major and trace element) characteristics of Bensa kaolin deposits in southern Ethiopia to assess the genesis and physico-chemical characteristics of Bensa kaolin.

2 GEOLOGY OF THE AREA

In this study kaolin mineral deposit is recognized in a place called Bensa which is a part of southern Ethiopia. Bensa locality is found 405km south of Addis Ababa, Ethiopia. Geologically the area are situated on two distinct geological formations, metamorphic terrains (from south) and volcanic terrains (from north), are joining each other. Southward dominant segments of study areas are covered by

Precambrain basemant rocks that comprising varies types of metamorphic rocks (like; Hornblende-Biotite schist, Biotite hornblende-quartz schist, Talc schist, Amphibolite, quartzo-feldspatic gneiss, Serpentine and other metasedimentary rocks) and their associated granitic intrusive rocks. Whereas, the remaining northward segment of the study area is covered by Cenozoic volcanic terrains of Ethiopia, which particularly dominated by continuous layers of volcanic pyroclastic deposits (Ignimbrite) and basaltic lava flow deposit (basaltic rocks). Genetically the kaolin deposit on both localities are regarded basically as a product of weathering alteration product of feldspar rich pyroclastic volcanic rocksThe Cenozoic volcanic rocks cover about 144km2 of the area. They are mostly dominated by continuous layers of basaltic lava flow and pyroclastic deposit (rhyolitic ignimbrite). The volcanic rocks of the area found directly overlying the basement metamorphic rocks. The lower parts of the volcanic sequences found to be gentle slope forming undulating topography with high degree of weathering, on the contrary the upper parts form steep cliff with columnar jointing strictures.

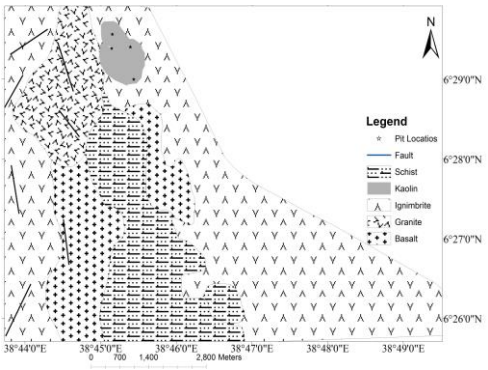

***Fig. 1**. Geological Map of Bensa area showing the general lithological distribution*

2.1 Geology of the host rock (Ignimbrite)

This rock unit is mostly exposed and covers the highland parts of the area. In some localities the ignimbrite unit is exposed following streams and rivers which clearly indicate that their deposition following lowlands. In some parts the ignimbrite unit is directly overlies the Precambrian basement rocks by forming cliff and columnar jointing strictures where lower basaltic unit is absent. Whereas in areas where the lower basalt is present this unit is directly overlies on the lower basaltic successions. Along the river of Logita and Gambelto this rock exposure is extensively overlying on the basement rock, following this river in some areas the exposure is interrupted due to intense erosion activity. In different places the unit shows variation in degree of welddness and fragment proportions.

3 METHODS

For this study major and trace element chemistry of the kaolin samples and the host rock petrography were analyzed. During field investigation 6 pits were dug to characterize the physical property of the kaolin deposit and to observe physical property variation of the kaolin with depth (color variation and texture). The pits location was selected from the northern periphery to the southern periphery of the deposit to see variation of the kaolin deposit across the whole area. 1 representative samples were collected from each of the six pits for both geochemical and engineering characterizations tests like; Durability, strength, water absorption, atterberg limit, hydrometer analysis, soundness and flakiness tests. Additionally to see the modal composition of the parent/host rock of the kaolin deposit petrographic analysis of the host rock were conducted. The six kaolin samples major and trace element were analyzed at ALS (Australian Laboratory service) Ireland, Doblin branch. The major elements were analyzed by XRF and trace elements were analyzed by ICP-MS. Accuracy and analytical procedure for both major and trace elements are available on the ALS official website [22] Engineering characterizations tests; durability, strength, water absorption, Atterberg limit test, hydrometer analysis, soundness and flakiness tests have been analyzed at Dilla University, Engineering and Technology college laboratory. Thin section preparation and petrographic analysis of the host/parent rock for the kaolin deposit were conducted in Geological Survey of Ethiopia, Addis Ababa laboratory.

4 RESULTS

4.1 Geology of the Kaolin Mineral Deposits

The kaolin deposit of Bensa area found to be a product of intense weathering of feldspar rich rhyolitic ignimbrite unit. Petrographic description of the ignimbrite (host rock) show dominant proportion of 7% elongated flat sanidine, 5% quartz, 5% large anhedral opaque and 2% plagioclase minerals and small proportion of Lithic fragment with the large proportion of volcanic glass (~76%) compose the rock. Glassy material is filling the interstices of Opaque, Sanidine, Quartz, Plagioclase and lithic grains. In the kaolin deposit of Bensa area small stream erodes the deposit around 20m thick kaolin. Several pits were dug on this kaolin deposit to characterize the deposit with in depth. Based on the data obtained from a 6m deep pit (pit-1, at the center) and pit-3 which is dug at 225m distant from pit-1 towards the northwestern direction, the kaolin shows white color, sticky and very fine grain texture with no variation in property up to 5m depth, but at 225m apart from pit-1 towards the southern margin of the deposit pit-2 was dug. In this pit, the kaolin shows dull color and coarser in grain size throughout depth. At the bottom of the pit-2 it was observed that the deposit tends to completely change into ash and lapilli size pyroclastic material. Pit samples from the center of the kaolin deposit shows (Pit-1, Pit-3 and Pit-5) shows white color very fine grain and sticky tough. But samples brought from the periphery of the deposit shows dull to reddish color with some grains of quartz. The physical characteristics of kaolin samples from different pits are presented in table 1 below.

***Table 1** Physical characteristics of Bensa kaolin from different pits with different location within the deposit*

Area	*Atterberg Limit*	
	Liquid limit (LL)	*Plastic limit(PL)*
Sample from the center	*37.92*	*NP*
Samples from the periphery	*63.82*	*83.33*

4.2 Physical property of the kaolin deposit

Hydrometer analysis of disturbed samples was carried out for Bensa kaolin deposits at Dilla University, engineering and technology college soil laboratory. Hydrometer analysis is an application of stokes' law that permits calculating the grain size distribution in silts and clays, where the soil particles are given the sizes of equivalent spherical particles. The grading characteristics of particles size shows that, clay fraction (<0.002mm) 10% and silt sized (0.002–0.074mm) particles are 18%.

Table 2 *showing the hydrometer analysis result of Bensa Kaolin*

Hydrometer (samples from the periphery)		Hydrometer (samples from the center)	
Grain size (mm)	Percent finer (%)	Grain size (mm)	Percent finer (%)
0.02415	12.59	0.02415	29.1
0.01548	18.78	0.01548	18.78
0.00922	13.83	0.00922	13.83
0.00663	10.94	0.00663	10.94
0.00475	10.52	0.00475	10.32
0.00104	8.83	0.00104	8.63

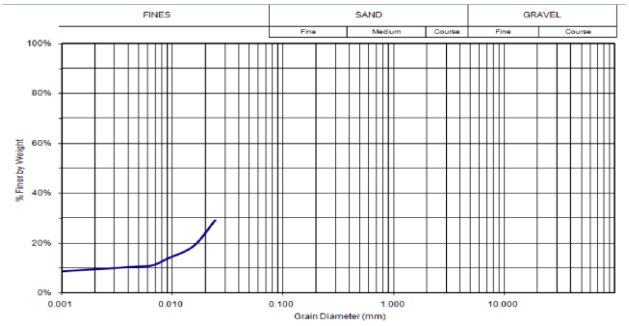

Fig. 2*. Graph showing grain size analysis of kaolin samples from the periphery of the deposit*

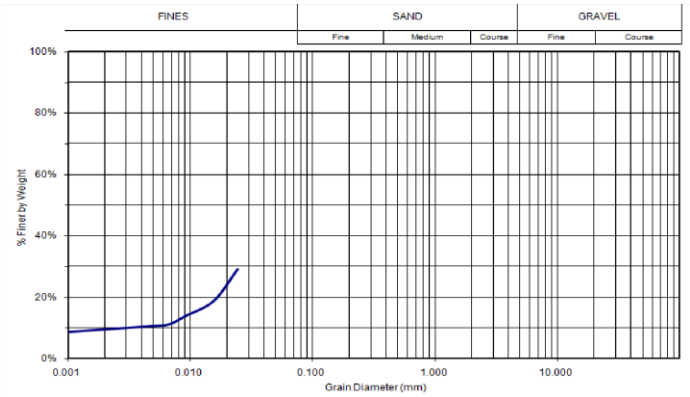

Fig. 3. *Graph showing grain size analysis of Bensa kaolin sample from center of the deposit*

The particle size distribution curve at fig.2 and fig.3 reveals that, the particle size increases from left to right. The curve is situated relatively higher up and to the left which indicates the sample is fine grained soil containing clay and silts. The classification based on particle size may be misleading for fine-grained soils. The behavior of such soils depends on the plasticity characteristics in addition to their particle size. For further kaolin characterization atterberg limit test was conducted according to ASTM-D 4318 and D-422 procedures for both area samples and the results are presented in table 3.

Table 3 *showing the Plasticity test results of Bensa area kaolin clay*

Pit No.	*Location*	*Pit depth*	*Color*	*Average Grain size*
pit-1, pit-3	*The center of the deposit*	*6m*	*Whitish*	*Very fine grained with sticky touch*
Pit-2, Pit-4 and Pit-6	*Periphery of the deposit*	*6m*	*Dull at the top and Whitish at the bottom*	*Fine at the top and becoming coarser at the bottom*
Pit-5	*From stream cut*	*20m*	*Whitish*	*Very fine grained with sticky touch*

During plastic limit testing, kaolin samples from the periphery of the deposit was easily rolled while samples from the center begins to crumble before rolling to a rod like 3mm thick thread shape. Therefore, the plastic limit of samples from the center could not be determined. A periphery sample has a plastic limit greater than its liquid limit. This indicates that the kaolin behaves a non-plastic (NP) characteristic. Therefore, according to the above specifications and atterberg limit test results kaolin deposits occur at both localities are clayey and non-plastic in nature.

4.3 Geochemical characteristics of Bensa Kaolin

4.3.1 Major element Geochemistry of Bensa Kaolin

Whole rock major and trace element composition of Bensa kaolin deposits are presented in table 3 bellow. On Winchester and Floyd [26] volcanic classification diagram (Nb/Y Vs $Zr/TiO_2x0.0001$) plot all samples fall in the field of Trachyte (fig.4) except samples KO-0 and KO-2 which falls in the field of trachyte Com/Pant boundary. These two samples are brought from the periphery of the deposit and physically characterized as coarse grain texture. The kaolin deposits in the area exhibits high concentration of SiO_2 ranges between 53.6 to 68.8 wt. % and Fe_2O_3 (4.85-7.74 wt. %). Iron oxide concentrations of the deposits are extensively exceeding the allowed limits of kaolin for industrial application (1 wt. % Fe_2O_3; [23]). The high concentrations of iron oxide in the deposits is probably due to the breakdown of opaque minerals during weathering from the parent ignimbrite rock which is consistent with the high modal proportions of opaque mineral in the parent/host rock (5 Vol. %). The deposit is characterized by low concentrations of Al_2O_3 (13.8 to 22.7 wt. %) which is very low compared with commercial grade ceramic value (37-38 wt. %; [23]). Highly mobile major element oxides concentrations are low compared with Fe_2O_3 in the deposits CaO (0.27-0.62 wt. %), MgO (0.14-0.31 wt. %), P_2O_5 (0.1-0.2 wt. %) and MnO (0.12-0.3 wt. %), which reflects a complete loss of this mobile element during kaolinisation processes. Major element Na_2O and SiO_2 vs

LOI variation diagram show a negative correlation trend against, whereas Al_2O_3 and Fe_2O_3 exhibits a linear positive trend on the variation diagram against LOI of kaolin deposits of the area (fig.5). On Al_2O_3 versus Fe_2O_3 and LOI versus Fe_2O_3 variation diagrams the plot shows a linear positive correlation trend against. The high concentration of Fe_2O_3 (4.85-7.74 wt. %) in all kaolin samples of the area and its positive correlation with Al_2O_3 and LOI on the variation diagram indicates intense oxidation of iron-titanium oxide minerals and the iron forms a more stable iron oxide for example goethite (αFeO.OH) in the kaolin samples of the area [25], [12].

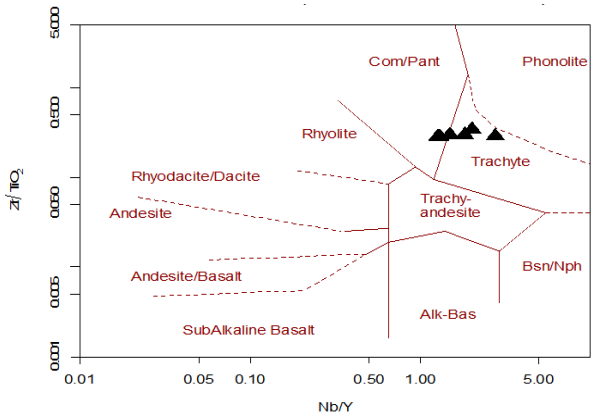

***Fig. 4**. Nb/Y Vs Zr/TiO_2 X 0.0001 plot after Winchester and [26] of Bensa and Koshe kaolin samples*

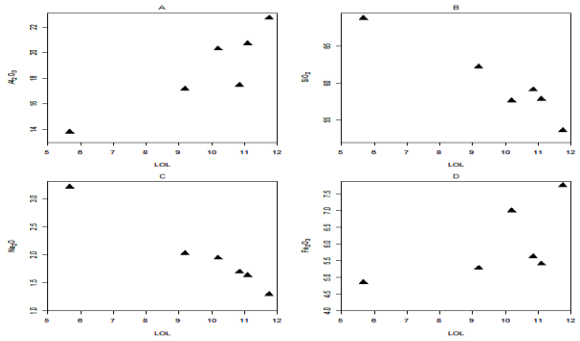

***Fig. 5**. Bensa kaolin samples major element versus LOI variation diagram*

***Table 4** Major and trace element composition of Bensa Kaolin*

Wt %	K2	K3	K4	KO-0	KO-2	KO-5
SiO_2	53.6	68.8	57.6	59.1	62.2	57.8
Al_2O_3	22.7	13.8	20.3	17.45	17.15	20.7
Fe_2O_3	7.74	4.85	6.98	5.62	5.27	5.4
CaO	0.29	0.27	0.27	0.53	0.48	0.62
MgO	0.21	0.14	0.18	0.31	0.25	0.22
Na_2O	1.29	3.2	1.94	1.69	2.02	1.63
K_2O	1.53	3.75	2	2.87	3.46	2.48
Cr_2O_3	<0.01	<0.01	<0.01	<0.01	<0.01	<0.01
TiO_2	0.61	0.38	0.56	0.49	0.45	0.51
MnO	0.3	0.19	0.26	0.16	0.12	0.13
P_2O_5	0.01	0.02	0.01	0.02	0.01	0.01
SrO	0.01	<0.01	<0.01	<0.01	<0.01	<0.01
BaO	0.06	0.02	0.04	0.07	0.06	0.05
LOL	11.75	5.67	10.2	10.85	9.19	11.1
Trace element PPM						
C	0.02	0.02	0.07	0.16	0.09	0.01
S	<0.01	<0.01	<0.01	<0.01	<0.01	<0.01
Ba	548	201	312	593	505	479
Ce	528	262	361	406	302	343
Cr	<10	<10	10	20	10	10
Cs	1.29	1.52	1.67	1.41	1.23	0.54
Dy	20	22.7	26.3	26.2	22.9	22
Er	12	13.65	14.75	15.85	13.1	12.45
Eu	2.38	2.56	2.97	4.69	3.72	3.91
Ga	58.8	35.8	53.3	43.5	43.7	54
Gd	19.95	23.8	25.8	26.9	22.9	22.9
Ge	<5	<5	<5	<5	<5	<5
Hf	44.6	26.8	38.5	35.5	33.1	45.4
Ho	3.96	4.51	5.11	5.3	4.73	4.41
La	128.5	135.5	156.5	169.5	146.5	139
Lu	1.79	1.91	2.14	2	1.72	1.58
Nb	230	143	209	181.5	178	219
Nd	124.5	138.5	152.5	169	144	134.5
Pr	35.2	35	40.8	44.1	37.1	35.6
Rb	32.3	88.4	44.2	76.2	81.1	55.9
Sm	24.9	25.8	29.3	32.9	27.7	27.4
Sn	12	8	12	11	10	13
Sr	28.4	25.7	29.4	28.5	23.3	60.5
Ta	14.5	9.3	12.7	11.5	11.3	14.8
Tb	3.31	3.71	4.3	4.24	3.72	3.68
Th	29.8	18.2	26.3	19.25	19.05	23.7
Tm	1.69	2.01	2.3	2.28	1.91	1.91
U	1.19	3.59	2.55	2.8	3.13	3.22
V	22	14	17	33	22	18
W	3	2	2	2	2	2
Y	83.3	113	114.5	138.5	119	108.5
Yb	12.55	13.3	15.1	14.6	12.65	12.15
Zr	1770	1070	1670	1380	1350	1750
As	0.4	0.7	1	1.7	0.8	0.8
Bi	0.16	0.05	0.13	0.12	0.09	0.2
Hg	<0.005	<0.005	<0.005	0.011	0.012	0.006

In	*0.214*	*0.073*	*0.182*	*0.152*	*0.139*	*0.138*
Re	*0.001*	*0.001*	*0.002*	*0.002*	*<0.001*	*0.002*
Sb	*0.09*	*0.07*	*0.09*	*0.11*	*0.07*	*0.06*
Se	*2*	*1.3*	*2.2*	*1.9*	*1.5*	*1.6*
Te	*0.03*	*0.02*	*0.01*	*0.03*	*0.01*	*0.01*
Ti	*0.44*	*0.19*	*0.39*	*0.23*	*0.14*	*0.17*
Ag	*<0.5*	*<0.5*	*<0.5*	*<0.5*	*<0.5*	*<0.5*
Cd	*<0.5*	*<0.5*	*<0.5*	*<0.5*	*<0.5*	*<0.5*
Co	*5*	*3*	*3*	*5*	*2*	*2*
Cu	*3*	*2*	*3*	*6*	*5*	*4*
Li	*30*	*20*	*30*	*30*	*30*	*30*
Mo	*1*	*4*	*1*	*3*	*4*	*3*
Ni	*6*	*3*	*5*	*16*	*11*	*19*
Pb	*26*	*11*	*23*	*18*	*16*	*14*
Sc	*10*	*7*	*10*	*5*	*4*	*4*
Zn	*252*	*257*	*302*	*210*	*206*	*200*

4.3.2 Trace element Geochemistry of Bensa Kaolin

LOI versus trace element variation diagrams for Bensa kaolin are presented in figure 6 bellow. On the variation diagram high field strength elements (HFSE) Zr and Nb show a positive linear correlation trend with LOI, which implies HFSE concentrations increase with increasing of degree of alteration. On the contrary large ion lithophile element (LILE) (Rb and Cs) with minor exception exhibits a decreasing pattern with LOI on a variation diagram, which is indicator of LILE leaching out from the system when degree of weathering becomes more intense. Large ion lithophile element (LILE) Sr (23.3-60.5ppm), Rb (32.3-88.4ppm), Ba (201-593ppm) and Cs (0.54-1.67ppm) shows depletion pattern on the Chondrite normalized spider plot (normalization value after R.N. Thompson [27]) (fig.7) in all samples of the area. LILE are highly sensitive element for secondary processes like weathering and kaolinisation of alkali feldspar rich source material. However hydrothermal alteration cannot fractionate LILE sensibly from the primary rock during kaolinisation processes [16], [17]. High field strength element (HFSE) Zr (1070-1770ppm), Hf (26.8-45.4ppm), Nb (143-30ppm), Ta (9.3-14.8ppm) and REE concentrations of Bensa kaolin samples exhibit enrichment pattern over LILE. HFSEs are immobile elements and therefore during weathering process there concentrations are not expected to be affected. On Chondrite normalized REE diagram Eu shows very strong negative anomaly. In most felsic rock the negative anomaly of Eu reflects the fractionation of plagioclase feldspar mineral from the magmatic system during the genesis of the parent rock for the kaolin deposit (ignimbrite of the area in this case). Eu is incompatible element for all phases except plagioclase. Therefore the negative anomaly of Eu in the REE diagram could also be the result of breakdown of plagioclase during kaolinisation processes and/or the effect of both processes. Chondrite normalized REE diagram shows depletion of LREE over HREE which is a characteristic of most felsic rock. Bensa kaolin enrichment of LREE over HREE in the Chondrite normalized REE diagram is probably the kaolin deposit of the area inhabits the source rock geochemical signature.

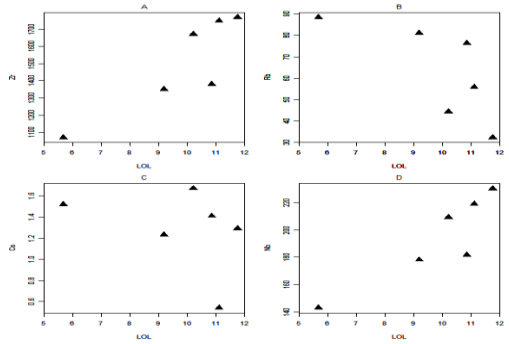

***Fig. 6**. Bensa kaolin samples trace element versus LOI variation diagram*

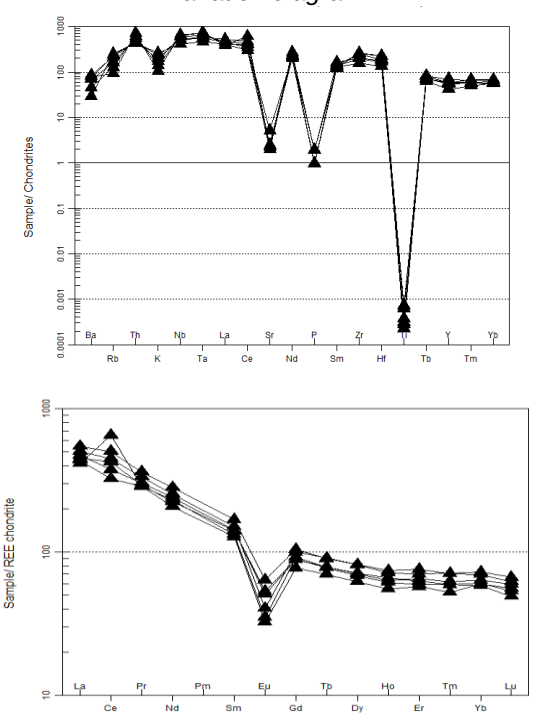

***Fig. 7**. Chondrite normalized spider diagram (normalization value after R.N. Thompson [27]) and Chondrite normalized REE diagram (Normalization value after W.V. Boynton [28]) of Bensa kaolin*

5 DISCUSSION

5.1 Alteration processes and element mobilization during kaolinisation

The very low K_2O/Al_2O_3 ratio in any kaolin deposit implies a complete kaolinisation of K-feldspar and micas, K_2O/Al_2O_3 ratio greater than 0.1 shows incomplete kaolinisation of K-feldspar and micas [12]. In Bensa kaolin sample K2 and k4 have K_2O/Al_2O_3 ratio <0.1 indicating a complete kaolinisation of k-feldspar and micas but the rest of the samples from the area show a range of K_2O/Al_2O_3 ratio (0.16-0.27) which is due to incomplete kaolinisation processes of k-feldspar and micas in the deposit. To evaluate the degree of alteration in the kaolin deposit chemical index of weathering (CIW) [14] and chemical index of alteration (CIA) [15] have been calculated

for Bensa kaolin deposit. CIW for Bensa kaolin deposit ranges from 79.9 % to 93.5 % and the CIA varies from 65.6 % to 87.9 % within the deposit. CIA versus CIW plot on a variation diagram can be used to determine the degree of silicate weathering [12]; the Bensa kaolin CIA vs. CIW plot sample number k3, ko-2 and ko-0 fall in the field of moderately silicate weathering area whereas sample ko-5, k5 and k2 fall on extreme silicate weathering field (figure 8). Samples characterized as moderately weathered silicate ko-2 and ko-0 are collected from the periphery of the kaolin deposit and k3 are collected from 20m deep stream cut and it is consistent with sandy grain physical property. Sample ko-5, k5 and k2 are brought from the middle of the deposit and its physical property is very fine sticky white color. The samples plot on the CIA vs. CIW diagram (after N. N. Bukalo et al. [12]) shows samples from the periphery and depth bellow 20m of the deposit shows low to moderate degree of silicate weathering; on the contrary samples from the middle of the deposit with less than 20m depth show a high degree of silicate weathering in the area.

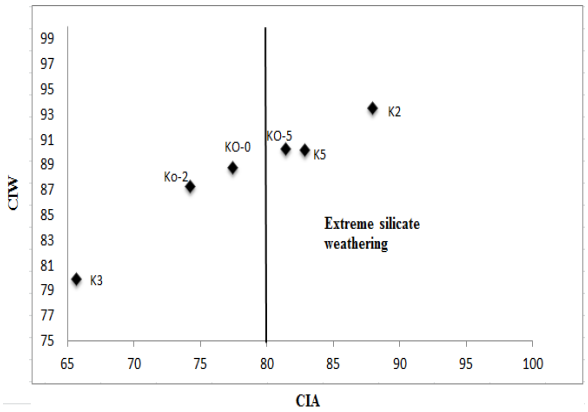

***Fig. 8**. Chemical index of alteration (CIA) versus chemical index of weathering (CIW) of Bensa kaolin plots area modified from N. N. Bukalo et al. [12]*

Supergene kaolinisation processes usually concentrate HFSE in the kaolin deposit and strongly deplete the immobile LILE [17], [29]. The Bensa kaolin deposit exhibits a very restricted value of LILE (Sr, 23.3-605ppm; Rb, 32.3-88.4ppm; Cs, 0.54-1.67 ppm). Feldspar alteration during kaolinisation processes release Ca, Na, K and Ba in to altering solutions [29], [30]. During weathering processes these highly mobile elements can be easily leached out from the system. Samples having coarse grain and dull color which brought from 20m deep stream cut exhibits relatively high concentration of SiO_2 (68.8 wt.%) whereas samples from the middle of the deposit shows depletion of SiO_2 (53.6-591 wt.%) and enrichment of Al_2O_3 (22.7 wt. %) and HFSE (Zr, Hf, Nb, Ta and REE). The contrasting pattern of HFSE and LILE between the more matured kaolin and immature/coarse grain sandy kaolin deposit in Bensa area reflects the intensity of weathering. HFSE Zr, Hf, Ta, Nb and REE are immobile during most alteration processes [31]. Therefore we conclude that the weathering processes during kaolinisation of Bensa kaolin deposit concentrates the HFSE and depletes the LILE in the kaolin. Degree of kaolinisation processes can be also estimated from the relationship between LOI and Al_2O3, SiO_2 on a variation diagram [32]. Strong linear positive correlation trend between LOI vs Al_2O and negative trend between LOI and SiO_2 on a variation diagram (fig.5) of Bensa kaolin reflects high degree of alteration concentrates Al_2O_3 and depletes SiO_2 in the kaolin deposit.

5.2 Genesis of the kaolin deposit

Depend on the processes involved during kaolinisation of a parent material the deposit can be hypogene or supergene kaolin [3], [4], [5], [6]. Hypogene kaolin is formed due to hydrothermal alterations of the parent material. Hydrothermal alteration principally concentrate LILE and a typical kaolin deposit formed by hydrothermal fluid have SiO_2/Al_2O_3 (1.04-1.45) [33], [29]. Bensa kaolin deposit shows SiO_2/Al_2O_3 ratio ranges between 2.36 and 4.98, Ce+Y+La (<739) and Ba+Sr (<622) this range of trace element is a characteristics of Supergene kaolin [34]. The very restricted value of P_2O_5 (0.01-0.02 wt. %), S (<0,01ppm; below the instrument detection limit) of Bensa kaolin deposit is consistent with its supergene origin, according to [35] hypogene kaolin deposit characterized by high concentrations and increment of P_2O_5, S and Sr with increment of degree of alteration. Bensa kaolin deposit geochemistry shows enrichment of HFSE, the very high Zr value of the deposit (1070-1770ppm) may reflects the alteration/weathering processes for Bensa kaolin occurred at low temperature. High temperature alteration sometimes cause mobilization of HFSE and can leach out Zr from the system and decrease its concentration in the deposit but low temperature alteration processes may concentrate Zr in the deposit [36]. REE diagram of Bensa kaolin deposit indicates extreme enrichment of LREE (eg. La, 128.5-169.5ppm; Ce, 262-528ppm) over HREE (Lu, 1.58-2.14ppm; Yb, 12.15-14.1ppm). All samples of the area have La/Lu ratios between (70-87) and $(La/Lu)_N$ ratio of greater than 1. The deposit contrasting pattern of LREE and HREE with depletion of Sr, Rb, Ba, P_2O_5, MnO and relatively high concentration of Fe_2O_3 and positive correlation of Fe_2O_3 with LOI on a variation diagram indicates that the parent rock for the kaolin deposit are weathering of felsic volcanic rock composed of plagioclase and Alkali feldspar in which the kaolinisation processes were the result of meteoritic fluids having low pH and low concentrations of carbonate species, or hydroxyl and halogens [37],[38], [39]..

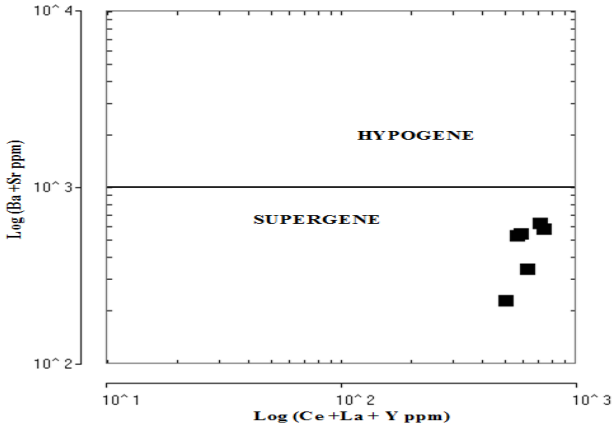

***Fig. 9**. Bensa kaolin samples on discrimination diagram of supergene-hypogene alteration of kaolin (fields are after H.G. Dill et al. [34])*

6 CONCLUSION

1. Physical and Geochemical properties (color, grain size of the kaolin and Al_2O_3 and SiO_2) of Bensa kaolin deposit shows maturity of the kaolin decrease with depth and towards the periphery of the deposit.
2. Bensa kaolin deposit geochemistry, enrichment of HFSE (Zr, Hf, Nb Ta and REE) and strong depletion of LILE (Rb, Sr, Ba and Cs) with SiO_2/Al_2O_3 ratio, high Ce+Y+La, low Ba+Sr and the very restricted value of P_2O_5 and S of the deposit indicates the kaolin genesis is supergene (weathering) of felsic volcanic rock composed of plagioclase and Alkali feldspar.
3. Contrasting pattern of LREE and HREE (high La/Lu ratio) with depletion of Sr, Rb, Ba, P_2O_5, MnO of Bensa kaolin indicates that the kaolinisation processes were the result of meteoritic fluids having low pH and low concentrations of carbonate species, or hydroxyl and halogens and the very high Zr value of the deposit (1070-1770ppm) may reflect the alteration/weathering processes for Bensa kaolin occurred at low temperature.
4. Relatively high concentration of Fe_2O_3 and positive correlation of Fe_2O_3 with LOI indicates the formation of more stable iron oxide in the kaolin deposit

7 ACKNOWLEDGMENT

We would like to give our deepest gratitude for Mr. Showa and Mr. Muhib and all staff members of Southern Nation Nationality and People of Ethiopia (SNNPE) Regional mine and energy office. This research was funded by Southern Nation Nationality and People of Ethiopia (SNNPE) Regional mine and energy office 2018 research grant.

8 REFERENCES

[1] O. Benjamin, A. Ebenezer, O. Ayodele, O. Joseph, U. Emmanuel, A.Thomas, Characterization of Kaolin Deposits in Okpella and Environs, Southern Nigeria. International Journal of Geosciences, 10: 317-327pp, 2019.

[2] N.E. Idenyi, C.O. Nwajagu, Non-Metallic Material Technology. Olison Publication, Enugu, 2003.

[3] H.H. Murray, Kaolin minerals: Their genesis and occurrences. In: bail Ey, s.w. (ed.): Hydrous phyllosilicates (Exclusive of micas). Reviews in Mineralogy, 19, Mineralogical Society of America, Washington, D.C, 1988.

[4] H.H. Murray, W.D. Keller, Kaolins, kaolins and kaolins. In: H.H. Murray, W.M. Bundy, C.C. Harvey, (Eds.), Kaolin Genesis and Utilization. The clay Minerals Society, Boulder, CO, pp. 1–24, 1993.

[5] H.A. Gilg, S.H. Lmeyer, H. Miller, S.M. Sheppard, Supergene origin of the lastarria kaolin deposit, south-central Chile and paleoclimatic implications. Clays and Clay Minerals, 47:2, 201-211, 199.

[6] S. Ismail, V. Husain, S. Anjum, Mineralogy and Genesis of Nagar Parker Kaolin Deposits, Tharparkar District, Sindh, Pakistan. Int. j. econ. environ. geol., 5(1):33-40pp, 2014.

[7] Gemechu Bedassa, Worash Getaneh, Binyam Hailu, Geochemical and mineralogical evidence for the supergene origin of kaolin deposits–Central Main Ethiopian Rift. Journal of African Earth Sciences, 149: 143–153pp, 2019.

[8] Bakari Ali, Zauro Tukur, Geochemical and Geological Characterization of Kaolinite Deposits around Kaoje, Kebbi State, Nigeria. International journal of scientific & technology research, 4/11: 97-100pp, 2015.

[9] F. Cravero, E. Domınguez, C. Iglesias, Genesis and applications of the cerro rubio kaolin deposit, patagonia (Argentina). Appl. Clay Sci. 18, 157–172, 2001.

[10] Njoya, C. Nkoumbou, D. Grosbois, D. Njopwouo, D. Njoya, A. Courtin-Nomade, J. Yvon, F. Martin, Genesis of Mayouom kaolin deposits (western Cameroon). Applied Clay Science 32, 125–140pp, 2006.

[11] Meyer, J.J. Hemley, Wall rock alteration. In: Barnes, H.L. (Ed.), Geochemistry of Hydrothermal Ore Deposits, 167–235pp, 1967.

[12] N. N. Bukalo, E. Georges-Ivo, E. Ekosse, O. John Odiyo, S. Jason, Geochemistry of Selected Kaolins from Cameroon and Nigeria, Review Article. Open Geosci; 9:600–612pp, 2017.

[13] Meunier, B. Velde ,P. Dudoignon, D. Beaufort, Identification of weathering and hydrothermal alteration in acidic rocks: petrography and mineralogy of clay minerals. Sci. Geol. Mem. 72: 93–99pp, 1983.

[14] L. Harnois, the CIW index: a new chemical index of weathering. Sediment Geol. 55, 319–322pp, 1988.

[15] H.W. Nesbitt, G.M. Young, Early Proterozoic climates and past plate motions inferred from major element chemistry of lutites. Nature 299, 715–717pp, 1982.

[16] J.A. Grant, The isocon diagram. A simple solution the Gresens' equation for metasomatic alteration. Econ. Geol. 81, 1986.

[17] J.C.F. Caliani, E. Galán, P. Aparicio, A. Miras, M.G. Márquez, Origin and geochemical evolution of the Nuevo Montecastelo kaolin deposit (Galicia, NW Spain). Applied Clay Science, 49:91–97pp, 2010.

[18] E. Dominguez, C. Iglesias, M. Dondi, The geology and mineralogy of a range of kaolins from the Santa Cruz and Chubut provinces, Patagonia (Argentina). J. Clay Sci. 40: 124-142pp, 2008.

[19] E.A. Dominguez, C. Iglesias, M. Dondi, H.H. Murray, Genesis of the La Espingarda kaolin deposit in Patagonia. Applied Clay Science, 47:290-302pp, 2010.

[20] T. Solomon, M. Jean-Pierre, D. Yves, Geology and mineral potential of Ethiopia: a note on geology and mineral map of Ethiopia. J. Afr. Earth Sci. 36, 273-313pp, 2003.

[21] Tibebu Mengistu and Haile Mickael Fentaw, The industrial mineral and rock resource potential of Ethiopia. Chron. Rech. Min. 540: 33-40pp, 2010.

[22] Australian Mineral Laboratory Service, Right Solutions, Right Partner Schedule of Services & Fees; Geochemistry, alsglobal.com, 52pp, 2019.

[23] D.E. Highley, China clay mineral dossier. British Geological Survey, UK, 26pp, 1984.

[24] A.J. Bloodworth, D.E. Highley, C.J. Mitchell, Industrial Mineral Laboratory Manual, Kaolin. Mineralogy and petrology group, British Geological Survey, United Kingdom, Nottingham, 80pp, 1993.

[25] K.S. Arifln, H.A. Rahman, H. Hussin K,A,A, Hadi, The

genesis and characteristics of primary kaolinitic clay occurrence at Bukit Lampas, Simpang Pulai, Ipoh, Bulletin of the Geological Society of Malaysia, 54: 9-16pp, 2008.
[26] J.A. Winchester, P.A. Floyd, Geochemical discrimination of different magma series and their differentiation products using immobile elements. Chemical Geology, 20: 245-252pp, 1977.
[27] R.N. Thompson, Magmatism of the British Tertiary volcanic province: Scot. Geol.18, 49-107pp, 1982.
[28] W.V. Boynton, Cosmochemistry of the Rare Earth Elements: Meteorite Studies. In: Henserson, P., Ed., Rare Earth Element Geochemistry. Elsevier, Amsterdam, 63-114pp, 1984.
[29] Ali Abedini and Ali Asghar, Geochemical characteristics of the Abgarm kaolin deposit, NW Iran. N. Jb. Geol. Paläont. Abh. 278/3:335-350pp, 2015.
[30] S.M. McLennan, S.R. Taylor, Sedimentary rocks and crustal evolution: tectonic setting and secular trends. J. Geol. 99: 1–21pp, 1991.
[31] N. Jiang, S. Sun, X. Chu, T. Mizuta, D. Ishiyama, Mobilization and enrichment of high-field strength elements during late- and post-magmatic processes in the Shuiquangou syenitic complex, Northern China. Chemical Geology, 200: 117-128pp, 2003.
[32] A.B. Searle, R.W. Grimshaw, the Chemistry and Physics of Clays. Inter-science Publishers, Inc., New York, 942pp, 1959.
[33] R.F.J. Giese, Kaolin minerals: Structures and stabilities. In: Bailey, S.W. (ed.): Hydrous phyllosilicates (Exclusive of micas). Reviews in Mineralogy, 19, Mineralogical Society of America, Washington, D.C. 1988.
[34] H.G. Dill, H.R. Bosse, H.R. Henning, A. Fricke, H. Ahrendt, Mineralogical and chemical variations in hypogene and supergene kaolin deposits in a mobile fold belt of the Central Andes of northwestern Peru. Mineralium Deposita, 32:149-163pp, 1997.
[35] Grecco, S. Marfill, P.J. Maiza, Mineralogy and geochemistry of hydrothermal kaolin's from the Adelita mine, Patagonia (Argentina); relation to other mineralization in the area. Clay Minerals, 47:131-146pp, 2012.
[36] S. Salvi, A.E. WilliaMs-Jones, The role of hydrothermal processes in concentrating high-field strength elements in the strange Lake peralkaline complex, northeastern Canada. Geochimica et Cosmochimica Acta, 60: 1917-1932pp, 1996.
[37] M. Bau, Rare earth element mobility during hydrothermal and metamorphic fluid-rock interaction and the significance of the oxidation state of europium. Chemical Geology, 93:219-230pp, 1991.
[38] M. Bau, P. Moller, Rare earth element fractionation in metamorphogenic hydrothermal calcite, magnesite and siderite. Mineralogy and Petrology, 45: 231-246pp, 1992.
[39] S. Kadir, H. Erkoyun, Genesis of the hydrothermal Karaçayır kaolinite deposit in Miocene volcanics and Palaeozoic metamorphic rocks of the Uşak-Güre Basin, western Turkey. Turkish Journal of Earth Sciences, 22: 444-468pp, 2013.